

# TWO-LAYER OPTIMAL SCHEDULING OF AC/DC HYBRID MICROGRID WITH PET

Shiqi Guo<sup>1</sup>, Yunfei Mu<sup>1\*</sup>, Wei Lin<sup>1,2</sup>, Hongjie Jia<sup>1</sup>, Tianjiao Pu<sup>3</sup>, Xiaodong Yuan<sup>4</sup>

1 Key Laboratory of Smart Grid of Ministry of Education (Tianjin University), Tianjin 300072, China

2 Economic Research Institute of State Grid Fujian Electric Power Company, Fuzhou 350012, China

3 China Electric Power Research Institute, Beijing 100192, China

4 Jiangsu Electric Power Research Institute, Nanjing 211103, China

## ABSTRACT

In this paper, an AC/DC hybrid microgrid with PET is firstly modeled, and then a two-layer optimization model is established with the objective of minimizing the operating cost of AC/DC hybrid microgrid. Finally, the above two-layer optimization model is converted to a single-layer optimization model through KKT method for solving. According to the analysis of the case, the scheduling method based on two-layer optimization considers the cost of purchasing the PET in the upper layer and the operating cost of the different microgrids in the lower layer, and realizes the flexible scheduling between the main grid and microgrids through PET. Compared with the AC/DC hybrid microgrid with AC/DC converter, the hybrid microgrid with PET has flexible power regulation characteristics, and has advantages in reducing operating costs, fully absorbing and efficiently utilizing the renewable energy.

**Keywords:** Power electronic transformer, AC/DC hybrid microgrid, Distributed energy resources, Double-layer optimal scheduling

## NONMENCLATURE

### Abbreviations

PET	Power electronic transformer
KKT	Karush–Kuhn–Tucker

### Symbols

$\eta$	The loss factor of PET
--------	------------------------

## 1. INTRODUCTION

In recent years, with the continuous development and application of renewable energy, more and more

distributed power generation devices are connected to the power grid. Many distributed power generation devices, such as photovoltaics and electric vehicles, are in the form of DC. However, due to historical reasons, the AC power grid is the main form of the current power grid. It is not feasible to convert the existing power grid into a DC system in a short period of time<sup>[1-3]</sup>.

In the traditional AC microgrid, the DC device is connected to the AC microgrid through the AC/DC converter. In AC/DC hybrid microgrid, the DC device can directly access the DC microgrid, which reduces the conversion link and improves the power transmission efficiency. The DC hybrid microgrid is in the development stage, and it is of great significance to optimize the AC/DC hybrid microgrid to achieve full absorption of renewable energy and economic operation of the hybrid microgrid.

The chaotic particle swarm optimization algorithm is applied to an AC/DC hybrid microgrid based on two-layer optimal scheduling model for source-storage coordination in [4]. A real-time electricity price mechanism is proposed to improve the economic benefits of AC/DC hybrid microgrid in [5]. A coordinated economic dispatching method for energy storage and converter stations of AC/DC hybrid microgrid based on safety constraints is proposed in [6]. The cultural genetic algorithm is applied to solve an AC/DC hybrid microgrid optimization operation problem in [7]. At present, the optimal scheduling for AC/DC hybrid microgrid mainly focuses on the innovation of the algorithm and the perfection of the energy storage model. For the bridge connecting the internal AC area and the DC area of the AC/DC hybrid microgrid, most of the papers use traditional AC/DC converters as energy transmission devices for AC and DC microgrids, while coordinated

scheduling for AC/DC hybrid microgrid with PET is rarely mentioned.

A PET consists of power electronics and high-frequency transformers. Compared with the original two-port converter, PET can be coupled to three or four ports, and the input and output ports are isolated by a high-frequency transformer<sup>[8-10]</sup>. Since PET is connected to multiple voltage-level grids and has power flow control capabilities, it is possible to achieve new energy consumption between different microgrids through PET and improve the scope of consumption.

In this paper, a two-layer optimal scheduling method for AC/DC hybrid microgrid with PET is proposed and solved by KKT method. According to the analysis of the case, the scheduling method based on two-layer optimization realizes the flexible scheduling between main grid and microgrids through PET. Compared with the AC/DC hybrid microgrid with AC/DC converter, the hybrid microgrid with PET has advantages in reducing operating costs, fully absorbing and efficiently utilizing the renewable energy.

## 2. AC/DC HYBRID MICROGRID MODEL

The structure of AC/DC hybrid microgrid with PET is shown in Fig.1. The AC/DC hybrid microgrid model is simplified as follows: (1) Distributed energy resources in the microgrid are uniformly modeled and equivalent to a large-capacity DG unit; (2) the loads in the AC microgrid are equivalent to a high-power AC load, and the load in the DC microgrid is equivalent to a high-power DC load.

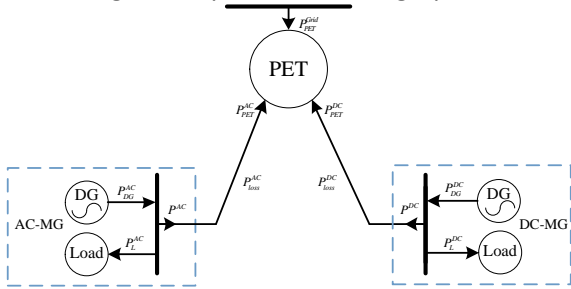


Fig.1 Structure of AC/DC hybrid microgrid with PET

Based on the above simplifications, the mathematical models of the AC microgrid and the DC microgrid have some similarities, including the power balance equation, the DG output constraint, and the load reduction constraint. Taking the AC microgrid as an example, its operational constraints are as shown in Eq.(1)-Eq.(3).

$$P^{AC} = P_{DG}^{AC} - P_L^{AC} + P_{IL}^{AC} \quad (1)$$

$$0 \leq P_{DG}^{AC} \leq P_{DG,max}^{AC} \quad (2)$$

$$0 \leq P_{IL}^{AC} \leq P_{IL,max}^{AC} \quad (3)$$

Where  $P^{AC}$  is the external transmission power of the AC microgrid;  $P_{DG}^{AC}$  is the output power of the DG in the AC microgrid;  $P_L^{AC}$  is the AC microgrid load power;  $P_{IL}^{AC}$  is the AC microgrid load reduction power;  $P_{DG,max}^{AC}$  is the maximum DG output in the AC microgrid;  $P_{IL,max}^{AC}$  is the maximum value of the load reduction power in the AC microgrid.

PET is the “electric energy router” between the AC microgrid, the DC microgrid and the main grid<sup>[11-12]</sup>. It can realize the interconnection between different microgrids and the power control of different ports. Taking a three-port PET as an example, its optimized scheduling model includes power balance equation and port power constraint, as shown in Eq.(4)-Eq.(7). The PET optimized scheduling model is as follows:

$$P_{PET}^{AC} + P_{PET}^{DC} + P_{PET}^{Grid} + \eta |P_{PET}^{AC}| + \eta |P_{PET}^{DC}| + \eta |P_{PET}^{Grid}| = 0 \quad (4)$$

$$\sqrt{P_{PET}^{AC2} + Q_{PET}^{AC2}} \leq S_{PET,max}^{AC} \quad (5)$$

$$P_{PET}^{DC} \leq P_{PET,max}^{DC} \quad (6)$$

$$\sqrt{P_{PET}^{Grid2} + Q_{PET}^{Grid2}} \leq S_{PET,max}^{Grid} \quad (7)$$

Where  $P_{PET}^{AC}$  is the power of the port connected to the PET and the AC microgrid, and inflowing PET is in the positive direction;  $P_{PET}^{DC}$  is the power of the port connected to the PET and the DC microgrid, and inflowing PET is in the positive direction;  $P_{PET}^{Grid}$  is the connected port of the PET and the main grid, and inflowing PET is in the positive direction,  $\eta |P_{PET}^{AC}|$ ,  $\eta |P_{PET}^{DC}|$ , and  $\eta |P_{PET}^{Grid}|$  are the power losses of the three ports of PET.  $S_{PET,max}^{AC}$  is the maximum apparent power of the port connected to AC microgrid;  $P_{PET,max}^{DC}$  is The maximum active power of the port connected to the DC microgrid;  $S_{PET,max}^{Grid}$  is the maximum apparent power of the port connected to the main grid.

## 3. TWO-LAYER OPTIMAL SCHEDULING MODEL

In this paper, PET and microgrid are considered to belong to different subjects. The two-layer optimization model is used to schedule PET and AC/DC hybrid microgrid. The model can take into account the optimization objectives of the upper and lower layers, and then rationally distribute the objective functions of different subjects.

### 3.1 Upper layer optimization model

The control variable of upper layer optimization is the power of each port of PET, and the objective function

is to minimize the purchase cost of PET, as shown in Eq.(8).

$$\min C_{PET} = \frac{(C_{ph} + C_{se})}{2} P_{PET}^{Grid} + \frac{(C_{ph} - C_{se})}{2} |P_{PET}^{Grid}| \quad (8)$$

Where  $C_{ph}$  is the price of PET purchasing electricity from the main grid;  $C_{se}$  is the price of PET selling electricity to the main grid.

The upper layer optimization constraints are shown in Eq.(4)-Eq.(7).

### 3.2 Lower layer optimization model

The lower layer optimization model focuses on the operating cost of the AC/DC microgrid, including two sub-optimization problems, namely, the minimization of the operating cost of the AC microgrid and the minimization of the operating cost of the DC microgrid. The control variable is the DG output and load reduction in the microgrid. Taking the AC microgrid as an example, the objective function of minimizing the running cost is as shown in Eq.(9).

$$\min C_{AC} = \frac{(C_{ph} + C_{se})}{2} (-P_{PET}^{AC}) + \frac{(C_{ph} - C_{se})}{2} |P_{PET}^{AC}| \quad (9)$$

$$+ C_{DG} P_{DG}^{AC} + C_{IL} P_{IL}^{AC}$$

Where  $C_{DG}$  is the operating cost of DG in the AC microgrid, and  $C_{IL}$  is the cost of the load reduction in the AC microgrid.

The constraints of the AC microgrid are shown in Eq.(1)-Eq.(3), and the constraints of the DC microgrid only needs to change the superscript from "AC" to "DC" in Eq.(1)-Eq.(3).

### 3.3 Two-layer optimization algorithm

The KKT method is used to rewrite the lower layer optimization problem in the two-layer optimization problem into the KKT conditional form, which is incorporated into the constraints of the upper layer optimization problem, thus transforming the two-layer optimization problem into a single-layer optimization problem. Taking the AC microgrid in the lower layer optimization as an example, the mathematical process of the KKT method is as follows: First, the AC microgrid constraint is rewritten as a standard form, as shown in Eq.(10)-Eq.(19), where  $\lambda_1^{AC}, \dots, \lambda_5^{AC}$  are the Lagrange multipliers corresponding to the constraints in the standard form respectively; secondly, the Lagrange function is written; finally, the Stationarity condition, the Primal feasibility condition, the Dual feasibility condition,

and the Complementary slackness condition involved in the KKT condition are written.

$$C_1^{AC} = P_{DG}^{AC} - P_L^{AC} + P_{IL}^{AC} - P^{AC} = 0: \lambda_1^{AC} \quad (10)$$

$$C_2^{AC} = P_{DG}^{AC} \geq 0: \lambda_2^{AC} \quad (11)$$

$$C_3^{AC} = -P_{DG}^{AC} + P_{DG,max}^{AC} \geq 0: \lambda_3^{AC} \quad (12)$$

$$C_4^{AC} = P_{IL}^{AC} \geq 0: \lambda_4^{AC} \quad (13)$$

$$C_5^{AC} = -P_{IL}^{AC} + P_{IL,max}^{AC} \geq 0: \lambda_5^{AC} \quad (14)$$

$$L^{AC} = C_{AC} - \lambda_1^{AC} (P_{DG}^{AC} - P_L^{AC} + P_{IL}^{AC} - P^{AC})$$

$$- \lambda_2^{AC} (P_{DG}^{AC}) - \lambda_3^{AC} (-P_{DG}^{AC} + P_{DG,max}^{AC}) \quad (15)$$

$$- \lambda_4^{AC} (P_{IL}^{AC}) - \lambda_5^{AC} (-P_{IL}^{AC} + P_{IL,max}^{AC})$$

$$\frac{\partial L^{AC}}{\partial P_{DG}^{AC}} = C_{DG} - \lambda_1^{AC} - \lambda_2^{AC} + \lambda_3^{AC} = 0 \quad (16)$$

$$\frac{\partial L^{AC}}{\partial P_{IL}^{AC}} = C_{IL} - \lambda_1^{AC} - \lambda_4^{AC} + \lambda_5^{AC} = 0 \quad (17)$$

$$\lambda_i^{AC} \geq 0 \quad \forall i = 2 \dots 5 \quad (18)$$

$$\lambda_i^{AC} C_i^{AC} = 0 \quad \forall i = 2 \dots 5 \quad (19)$$

For the DC microgrid, the transformation process whose constraints are rewritten as the standard form is the same as above, and only the superscript "AC" in Eq.(10)-Eq.(19) needs to be changed to "DC".

## 4. CASE STUDIES

The structure of AC/DC hybrid microgrid with PET is shown in Fig.1. In order to highlight the optimization effect of AC/DC hybrid microgrid with PET, the proposed method is also applied to the tradition AC/DC hybrid microgrid. The system structure of tradition hybrid system is shown in Fig.2. In order to distinguish between the two structures, the variables involved in the hybrid microgrid with PET have the superscript "1"; the variables involved in the tradition hybrid microgrid have the superscript "2".

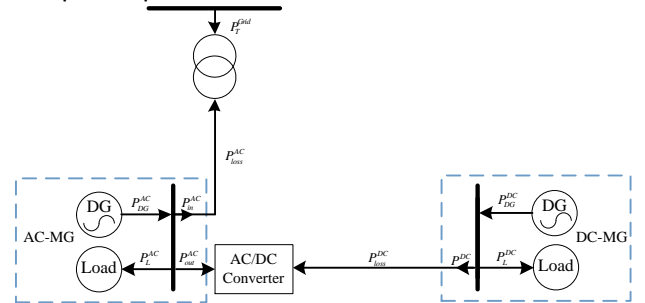


Fig.2 Structure of tradition AC/DC hybrid microgrid

Considering the different operating states of PET, four different simulation scenes are set. Scene I represents that the maximum DG output in the AC/DC microgrid is greater than the load; the scene II represents that the maximum DG output in the AC/DC microgrid is

less than the load; Scene III and scene IV represent that one microgrid in the power surplus state, and the other microgrid is in the power shortage state. The maximum DG output and microgrid load values in the hybrid microgrid in the four scenes are shown in Tab.1. In addition, it is assumed that the maximum load reduction amount is 10% of the load value. The values of other variable parameters involved in the simulation are shown in Tab.2.

Tab.1 AC/DC hybrid microgrid operating parameters in four simulation scenes

Scene number	AC microgrid		DC microgrid	
	DG output maximum	Load	DG output maximum	Load
Scene I	4MW	3.5MW	4 MW	3.5MW
Scene II	4 MW	5 MW	4 MW	5 MW
Scene III	4 MW	5 MW	5 MW	4 MW
Scene IV	4 MW	3.5MW	3.5 MW	4 MW

Tab.2 AC/DC hybrid microgrid simulation parameters

Parameter	Value
PET loss factor $\eta$	0.02
Maximum apparent power of the port connected to PET and AC microgrid $S_{PET,max}^{AC}$	2MW
The maximum active power of the port connected to the DC microgrid $S_{PET,max}^{DC}$	2MW
Maximum apparent power of the port connected to the main grid of PET $S_{PET,max}^{Grid}$	2MW
AC microgrid voltage $U_{AC}$	380V
DC microgrid voltage $U_{DC}$	375V
Line unit impedance $z$	0.642+j0.101Ω/km
Line length $l$	200m
Purchase price $C_{ph}$	59.21\$/MWh
Electricity price $C_{se}$	47.37\$/MWh
DG operating cost $C_{DG}$	20\$/MWh
Load reduction cost $C_{IL}$	41\$/MWh

Tab.3 Comparison of optimization results in four simulation scenes

Scene number	With PET			With AC/DC converter		
	$C_{PET}^1/\$$	$C_{AC}^1/\$$	$C_{DC}^1/\$$	$C_T^2/\$$	$C_{Ad}^2/\$$	$C_{od}^2/\$$
Scene I	-23.63	54.09	56.32	-7.49	61.35	70
Scene II	82.52	130.11	130.11	205.83	138.39	130.11
Scene III	35.94	130.11	52.63	17.06	130.11	65.01
Scene IV	-8.52	56.32	92.32	-7.49	58.48	92.32

The proposed method is used to optimize the AC/DC hybrid microgrid as shown in Fig.1 and Fig.2, and the

objective function values in the four simulation scenes are shown in Tab.3. The data in Tab.3 is the operating cost of different microgrids in different scenes. The positive number represents the operating cost, and the negative number represents the operating profit. In the table:  $C_T^2$  is the power purchase cost of the transformer in the AC/DC hybrid microgrid with AC/DC converter, and is compared with the  $C_{PET}^1$ . It can be seen from the results that under the conditions of scene I, scene II and scene IV, the three objective function values of the AC/DC hybrid microgrid with PET are superior to the AC/DC hybrid microgrid with AC/DC converter; Under the scene III, the hybrid microgrid with PET and AC/DC converters have different optimization results for different objective functions. The specific analysis is as follows:

(1)Scene I: The maximum DG output in the AC/DC microgrid is greater than the load value. Therefore, both the AC microgrid and the DC microgrid are in the outward power transmission state, so the objective functions  $C_{PET}$  and  $C_T$  are both negative values. At the same time, considering that in the hybrid microgrid system with AC/DC converter, the DC microgrid needs to be transmitted through the AC microgrid line, so the loss is increased and the  $C_T^1$  is greater than  $C_{PET}^1$ . In addition, in the hybrid microgrid system with PET, the AC/DC microgrid can realize the connection with the superior distribution system through PET, which reduces the loss of the transmission power on the line, which is beneficial to the efficient use of DG output. , reducing the objective function values of  $C_{AC}^1$  and  $C_{DC}^1$ .

(2)Scene II: The maximum DG output in the AC/DC microgrid is less than the load value. Therefore, both the AC microgrid and the DC microgrid are in the state of purchasing electricity from the distribution system. Considering that the power shortage of the DC microgrid needs to be satisfied by the transmission of the AC microgrid line, the power loss of the line is increased. Therefore, the power of the hybrid microgrid system with AC/DC converter from the distribution system will be greater than the PET. In the case of the scene II, the objective function value of  $C_{PET}^1$  and  $C_{AC}^1$  in the hybrid microgrid system with PET is smaller than the objective function value of  $C_T^2$  and  $C_{AC}^2$  in the hybrid microgrid system with AC/DC converter. In addition, in the hybrid microgrid system with PET and AC/DC converter, the DC microgrid is at the end of power transmission. Therefore, the operating cost of the DC

microgrid is the same in both cases, that is, the objective function value  $C_{DC}^1$  and  $C_{DC}^2$  is equal.

(3)Scene III: The AC microgrid is in the power shortage state, and the DC microgrid is in the power surplus state. Therefore, the DC microgrid will transmit power to the AC microgrid, and at the same time, the power of the two systems cannot be completely matched. The system is supplemented. Considering that in a hybrid microgrid system with PET, the DC microgrid needs to transmit power to the AC microgrid through PET and the line, and the electrical distance is greater than that of the hybrid microgrid system with AC/DC converter. The power value transmitted from the PET to the AC microgrid is greater than the power value transmitted by the power frequency transformer to the AC microgrid, thereby causing the objective function value  $C_{PET}^1$  to be greater than the  $C_T^2$ . Correspondingly, the power value transmitted from the DC microgrid to the AC microgrid in the hybrid microgrid system with PET is smaller than that of the hybrid microgrid system with AC/DC converter, thereby causing the  $C_{DC}^1$  to be smaller than the  $C_{DC}^2$ . In addition, in the hybrid microgrid system with PET and AC/DC converter, the AC microgrid is at the end of power transmission, so the operating cost of the AC microgrid is the same in both cases, that is, the objective function value  $C_{AC}^1$  and  $C_{AC}^2$  is equal.

(4)Scene IV: The AC microgrid is in the power surplus state, and the DC microgrid is in the power shortage state. Therefore, the AC microgrid will transmit power to the DC microgrid, and at the same time the power of the two systems cannot be completely matched. The system is supplemented. Considering that the difference between the maximum DG output and the load value (0.5 MW) in scene IV is smaller than the difference (1 MW) in scene III, the AC/DC hybrid microgrid will transmit power to the distribution system in the optimization result of scene IV. Therefore, the objective function values  $C_{PET}^1$  and  $C_T^2$  are both negative values. Since the electrical distance between the AC/DC microgrid is larger than that of the hybrid microgrid system with AC/DC converter in the hybrid microgrid system with PET, the power value of the AC microgrid to the PET is greater than that of the AC. The power value delivered by the microgrid to the power frequency transformer causes the objective function value  $C_{PET}^1$  to be less than  $C_T^2$ . Under the condition that the power shortage of DC microgrid is satisfied, the

sales of AC microgrid in the hybrid microgrid with PET is greater than that of the system with AC/DC converter, so  $C_{AC}^1$  is slightly smaller than  $C_{AC}^2$ . In addition, in the hybrid microgrid system with PET and AC/DC converter, the DC microgrid is at the end of power transmission, so the operating cost of the DC microgrid is the same in both cases, and the objective function value  $C_{DC}^1$  is equal to  $C_{DC}^2$ .

In order to further study the effect of hybrid microgrid with PET and hybrid microgrid with AC/DC converter in new energy consumption, the DG output of AC/DC microgrid under four simulation scenes is listed, such as Tab.4 and Tab.5 are shown.

Tab.4 DG output of AC/DC hybrid microgrid with PET in four simulation scenes

Scene number	With PET			
	$P_{DG}^{AC1}$ /MW	$\eta^{AC1}$	$P_{DG}^{DC1}$ /MW	$\eta^{DC1}$
Scene I	4	1	4	1
Scene II	4	1	4	1
Scene III	4	1	5	1
Scene IV	4	1	3.5	1

Tab.5 DG output of AC/DC hybrid microgrid with AC/DC converter in four simulation scenes

Scene number	With AC/DC converter			
	$P_{DG}^{AC2}$ /MW	$\eta^{AC2}$	$P_{DG}^{DC2}$ /MW	$\eta^{DC2}$
Scene I	3.8	0.95	3.5	0.875
Scene II	4	1	4	1
Scene III	4	1	4.5	0.9
Scene IV	3.9	0.975	3.5	1

Where  $\eta^{AC}$  and  $\eta^{DC}$  are respectively calculated by Eq.(20)-Eq.(21).They are used to characterize the degree of consumption of new energy in AC microgrid and DC microgrid. The closer the value is to 1, the higher the level of consumption of new energy.

$$\eta^{AC} = P_{DG}^{AC} / P_{DG,max}^{AC} \quad (20)$$

$$\eta^{DC} = P_{DG}^{DC} / P_{DG,max}^{DC} \quad (21)$$

It can be seen from the results that in the four simulation scenes of the AC/DC hybrid microgrid with PET, the DG is based on the maximum output, and the values of  $\eta^{AC}$  and  $\eta^{DC}$  are both 1.The AC/DC hybrid microgrid with AC/DC converter has different DG output situations under different simulation scenes. The specific performance is as follows: The hybrid microgrid system with AC/DC converter is only under scene II, the value of

$\eta^{AC}$  and  $\eta^{DC}$  is 1; Under scene I, scene III and scene IV, there is a phenomenon of waste of new energy. Therefore, in the three simulation scenes, the objective function values  $C_{AC}^2$  and  $C_{DC}^2$  in the hybrid microgrid system with AC/DC converter are greater than or equal to the objective function values  $C_{AC}^1$  and  $C_{DC}^1$  in the hybrid microgrid with PET. Therefore, the hybrid microgrid system with PET has a stronger advantage in terms of achieving full consumption and efficient utilization of new energy sources than the hybrid microgrid with AC/DC converter.

## 5. CONCLUSION

By optimizing the hybrid AC/DC microgrid with PET constructed in the four simulation scenes and comparing it with the traditional AC/DC hybrid microgrid, the following conclusions can be drawn:

(1) The scheduling method based on two-layer optimization considers both the cost of PET in the upper layer optimization model and the operating cost of different microgrids in the lower layer optimization model, and realizes flexible scheduling between PET and AC/DC microgrids.

(2) Compared with the AC/DC hybrid microgrid with AC/DC converter, the hybrid microgrid system with PET has flexible power regulation characteristics, which have advantages in reducing operating costs, fully absorbing and efficiently utilizing new energy sources.

## ACKNOWLEDGEMENT

This work was financially supported by the National Key Research and Development Foundation of China (2017YFB0903300).

## REFERENCE

- [1] Li Peng, Han Pengfei, Chen Anwei, Zheng Miaomiao. Fuzzy stochastic optimization operation of AC/DC hybrid microgrid with high density intermittent energy[J]. Proceedings of the CSEE, 2018, 38(10): 2956-2965.
- [2] Baranwal R, Castelino GF, Iyer K, et al. A Dual Active Bridge Based Single Phase AC to DC Power Electronic Transformer With Advanced Features[J]. IEEE Transactions on Power Electronics, 2018, PP(99):1-1.
- [3] Pu Tianjiao, Li Wei, Chen Naishi, Sun Yingyun, Mu Yunfei, Dong Lei, Kong Li. Key Technology and Research Framework of Optimized Operation Control of AC/DC Hybrid System Based on Power Electronic Transformer[J]. Power System Technology, 2018, 42 (09): 2752-2759.
- [4] Kang Chongqing, Yao Liangzhong. Key scientific issues and theoretical research framework for power systems

with high proportion of renewable energy[J].Automation of Electric Power Systems, 2017, 41(9): 2-11.

[5] Wang Chengshan, Li Peng, YuHao. Development and characteristic analysis of flexibility in smart distribution system[J].Automation of Electric Power Systems, 2018, 42(10): 13-21.

[6] Leng Xiwu, Chen Guoping, Bai Jingjie, Zhang Jiaqi. Overall design of big data analysis system for smart grid monitoring operation[J].Automation of Electric Power Systems,2018,42(12):160-166.

[7] Cao Yijia, Li Qiang, Tan Yi, et al. A comprehensive review of Energy Internet: basic concept, operation and planning methods, and research prospects[J]. Journal of Modern Power Systems and Clean Energy, 2018, 6(3): 399-411.

[8] Miranbeigi M, Iman-Eini H. Hybrid modulation technique for grid-connected cascaded photovoltaic systems[J]. IEEE Transactions on Industrial Electronics, 2016, 63(12): 7843-7853.

[9] Jiepin Z, Jianqiang L, Jingxi Y, et al. A Modified DC Power Electronic Transformer Based on Series Connection of Full-Bridge Converters[J]. IEEE Transactions on Power Electronics, 2018:1-1.

[10] Zhang Xianglong, Zheng Qiaohua, Zhang Dongying, Liu Ying. Optimization of AC/DC distribution system scheduling for power electronic substation[J]. Power System Technology, 2018, 42(11): 3718-3724.

[11] Li Zixin, Gao Fanqiang, Zhao Cong, Wang Zhe, Zhang Hang, Wang Ping, Li Yaohua. Summary of Power Electronic Transformer Technology Research[J]. Proceedings of the CSEE, 2018, 38(05): 1274-1289.

[12] Battistelli C, Agalgaonkar Y P, Pal B C. Probabilistic dispatch of remote hybrid microgrids including battery storage and load management[J]. IEEE Transactions on Smart Grid, 2016, PP(99): 1-1.